Influence of surface chemistry on ibuprofen adsorption and confinement in mesoporous silicon microparticles

Ermei Mäkilä[1,2], Henri Kivelä[3], Neha Shrestha[2], Alexandra Correia[2], Martti Kaasalainen[1], Edwin Kukk[4], Jouni Hirvonen[2], Hélder A. Santos[2], Jarno Salonen[1,]*

[1] Laboratory of Industrial Physics, Department of Physics and Astronomy, University of Turku, Turku, FI-20014, Finland

[2] Division of Pharmaceutical Chemistry and Technology, Faculty of Pharmacy, University of Helsinki, Helsinki, FI-00014, Finland

[3] Laboratory of Materials Chemistry and Chemical Analysis, Department of Chemistry, University of Turku, Turku, FI-20014, Finland

[4] Materials Physics Laboratory, Department of Physics and Astronomy, University of Turku, Turku, FI-20014, Finland

KEYWORDS porous silicon, drug delivery, confinement, interaction, nanocrystalline

ABSTRACT The effect of adsorption and confinement on ibuprofen were studied by immersion loading the molecules into mesoporous silicon (PSi) microparticles. The PSi microparticles were modified into thermally oxidized (TOPSi) and thermally hydrocarbonized (THCPSi), in order to evaluate the effects of the loading solvent and surface chemistry on the obtainable drug payloads. The payloads, location, and the molecular state of the adsorbed drug were evaluated using thermal analysis. The results showed that after ~800 mg/cm^3 (w_{drug}/V_{pores}) of drug had adsorbed into the mesopores, depending on the solvent used in the immersion, the drug began to rapidly recrystallize on the external surface of the particles. Moderate concentrations, however, enabled payloads of 800−850 mg/cm^3 without excessive surface crystallization, and thus, there was no need for rinsing the samples to remove the external crystallized portion. The results showed that the confined ibuprofen forms nanocrystals inside the mesopores after ca. 200 mg/cm^3 payloads were obtained, accounting for half of the adsorbed drug amount. The presence of both crystalline and non-crystalline phase was further characterized with variable temperature solid-state nuclear magnetic resonance (NMR) measurements. The interactions between the drug molecules and the pore walls of TOPSi and THCPSi were observed with Fourier transform infrared (FTIR) and ^{1}H NMR spectroscopies, and confirmed the hydrogen bonding between the silanol groups of TOPSi and the adsorbed ibuprofen, but having only limited effect on the overall state of the confined drug. *In vitro* drug permeation studies in Caco-2 and Caco-2/HT29 co-cultures showed the adsorption into hydrophilic or hydrophobic PSi microparticles had no significant effects on the ibuprofen permeation, whether the drug was partially nanocrystalline or completely in liquid-like state.

1 Introduction

Recent years have shown a growing interest for new methods in drug delivery to enhance the aqueous solubility and permeability of different therapeutic molecules in response to the continuous trend of new drug candidates toward larger and increasingly insoluble entities.[1,2] Poor dissolution characteristics can lead to insufficient and unpredictable bioavailability, making especially oral drug delivery difficult.[3] Proposed solutions are sought often with crystal engineering, which provides a powerful set of tools to address the poor solubility through, *e.g.* polymorph selection, size reduction and amorphization.[3–5]

Another possible solution is the application of mesoporous materials as drug carriers. These materials present remarkable versatility in their applications, especially in the cases of porous silicas and porous silicon (PSi), ranging from catalysis to sensors, and energy storage.[6–8] A broad overlap is seen in drug delivery, as both the materials have been shown to be effective in enhancing the solubility and permeability of poorly water-soluble drugs and in addition in providing protection and controlled release properties to larger and well soluble molecules, such as peptides and proteins.[9–19] The use of mesoporous carriers in drug delivery, however, requires broad understanding on how the carrier material affects the properties of the adsorbed payload.

A common factor for the mesoporous materials is the high available surface area, often in excess of several hundreds of m^2/g. The presence of grafted or native functional groups, provide multiple sites of interaction for the adsorbed molecules through *e.g.* hydrogen bonding.[20–24] Adsorption of molecules inside the mesopores can be used to exert control over the solid-state properties of the adsorbate. Physical confinement inside pores having diameter of 10–20× the size of the adsorbed molecules, has been shown to allow control over specific polymorph nucleation within the mesopores or the complete suppression of crystallization, rendering the adsorbate amorphous.[25–28] As the adsorbed molecules reside in either nanocrystalline or non-crystalline state, their thermodynamic properties are considerably different from bulk crystals, which can significantly enhance the aqueous solubility of the drug.

Depending on the surface chemistry of the adsorbent, the confined drug molecules often have liquid-like behavior, even at room temperature.[22,29] Strong interactions with the surface, however, could limit the

confinement effects, and leave the molecules in more solid-like rigid state.[30] Dielectric relaxation spectroscopy and solid-state nuclear magnetic resonance (NMR) results on mesoconfined ibuprofen have suggested that the combination of confinement and adsorbent surface interactions can lead to the presence of two groups of molecules with differing mobilities, depending on their location within the pore.[31,32]

The present work compares the behavior of ibuprofen adsorbed inside PSi microparticles. PSi was selected as the carrier since its branching, mesoporous structure with rough walls differs from the ordered silica-type materials and due to its silicon hydride terminated initial surface, that enables simple gas phase surface modifications.[33,34] Here, the PSi microparticles were stabilized into either hydrophilic thermally oxidized PSi (TOPSi) or hydrophobic thermally hydrocarbonized PSi (THCPSi). The two surface modifications allow the observation on how the presence or absence of hydrogen bonding capable silanol groups affect both the adsorption and confinement of ibuprofen. Three different solvents with solution concentrations ranging from low to nearly saturated were used. These are used to show that the selection of solvent and solution drug concentration can be used to control the drug adsorption process to obtain both a high confined drug payload, while keeping the excess drug from crystallizing on the outside of the carrier material low. The effect of the surface chemistry was also studied with regards to the molecular dynamics of the adsorbed ibuprofen, using thermal analysis and variable temperature solid-state NMR, as the selected pore size enabled the presence of nanocrystalline and amorphous-like phase concurrently inside the mesopores.[10,35] The effects of the PSi surface chemistry and the presence of nanocrystalline ibuprofen were studied with *in vitro* permeation experiments using cell lines for simulating the conditions of the gastrointestinal tract.

2 Experimental

2.1 Fabrication of PSi Microparticles

The PSi microparticles were fabricated as described in detail in the Supporting information. The microparticles between 25–75 μm were selected for the study and passivated into thermally oxidized PSi (TOPSi) and thermally hydrocarbonized PSi (THCPSi).

2.2 Drug Loading

The microparticles were loaded with ibuprofen (Orion Corp., Finland) using an immersion method. Different amounts of the drug were dissolved into ethanol (EtOH; 99.5 %, Altia Corp., Finland), chloroform (CHF; Merck GmbH, Germany) and tetrahydrofuran (THF; BDH Prolabo, USA). PSi microparticles were added with a ratio of 50 mg of PSi per 1 mL of added solvent. The loading process was done at room temperature using a gentle magnetic stirring. The loaded particles were removed from the solution by vacuum filtration after which they were dried at 65 °C for 20 h and, finally, stored in a silica desiccator at room temperature.

2.3 Characterization

2.3.1 Structural Properties

The structural characteristics of the PSi microparticles were determined with N_2 sorption at −196°C using TriStar 3000 (Micromeritics Inc., USA). The specific surface area (SSA) was calculated using the Brunauer-Emmet-Teller (BET) theory, while the pore volume was determined from the total adsorbed amount at a relative pressure p/p_0 = 0.97. Pore size distribution was calculated from the isotherm adsorption branch using the Barrett-Joyner-Halenda (BJH) theory. Scanning electron microscope (SEM) images of the PSi microparticles and of the porous layer cross-section were taken with Zeiss Sigma VP field-emission SEM (Carl Zeiss AG, Germany).

The water contact angle (WCA) of the two surface chemistries was estimated by placing a 5 μL droplet on a mesoporous PSi film, followed by taking a photograph of the sessile drop with a digital SLR camera

(Nikon D500), and analyzing the image with Geogebra 4.2. The PSi films used for the WCA estimation were collected prior to the ball milling and passivated using the same parameters as the microparticles.

2.3.2 Thermal Analysis

The total payload of the drug in the samples was determined with thermogravimetry (TG) using TGA-7 (PerkinElmer, USA) by placing ca. 4–6 mg of sample on platinum crucible and using a temperature ramp from room temperature to 800 °C at 40 °C/min under a constant N_2 flush of 200 mL/min. The weight loss observed for empty THCPSi particles and TOPSi particles was subtracted from the respective results. The drug payload is reported as w_{drug}/V_{pores} in mg/cm^3, *i.e.* the amount of drug vs. the available pore volume of the corresponding sample.

The physical state of the drug in the samples was characterized with differential scanning calorimetry (DSC) using Pyris Diamond DSC (PerkinElmer). The temperature and enthalpy scale was calibrated using an indium reference. Approximately 2–4 mg of sample was crimped into Al pans with holes and heated twice from 10 to 100 °C at 10 °C/min, with the latter run used as a sample baseline. The furnaces were flushed with N_2 at 40 mL/min. The DSC samples were stored for at least 2 months to allow possible recrystallization processes to proceed near completion.[35] Both the TG and DSC measurements were carried out at least in duplicates.

2.3.3 FTIR Spectroscopy

The infrared spectra of the PSi samples were determined using a Mattson Galaxy 6020 spectrometer (USA) equipped with a PA301 photoacoustic detector (Gasera Ltd., Finland). The FTIR mirror velocity was set to 0.6 cm/s and He was used as the detector chamber gas. The spectra were obtained averaging 32 scans.

2.3.4 NMR Spectroscopy

Variable temperature solid-state ^{1}H and ^{13}C NMR spectra were measured using a Bruker Avance 400 spectrometer with a 4 mm MAS (magic angle spinning) probe. The temperature calibration for the

measurements was done by observing the ^{207}Pb chemical shifts of $Pb(NO_3)_2$.[36] The detailed measurement protocols and pulse sequences are described in the Supporting Information.

2.4 Permeability Studies

The permeability studies were carried out on Caco-2 cells and on Caco-2/HT29 cocultures. The amount of released ibuprofen was determined with high performance liquid chromatography using Agilent 1260 HPLC. The culturing and HPLC protocols are explained in detail in the Supporting information.

3 Results and Discussion

3.1 Structural Characterization of PSi

The fabricated PSi microparticles were sieved into 25–75 μm size range due to its suitability for further formulation processing,[37] and passivated into either THCPSi or TOPSi, in order to prevent adverse reactions with the solvents or the solute.[33] The porous structure of the surface passivated materials is shown in Figure 1a, where the isotherm in both the cases displayed hysteresis loop, typical for mesoporous materials. The SSA of THCPSi and TOPSi, were 270 ± 14 m^2/g and 238 ± 2 m^2/g, respectively. Similar differences were observed in the total pore volumes, showing 1.01 ± 0.02 cm^3/g and 0.81 ± 0.01 cm^3/g for THCPSi and TOPSi, respectively. SEM images of the PSi layer cross-section and the microparticles are presented in Figure S1 (Supporting information).

The pore size distributions shown in Figure 1b indicated that the materials have a relatively narrow pore size distribution with an approximate average pore diameter of 10 nm, which compared to the size of an ibuprofen molecule (1.1×0.6 nm) is large enough to enable the drug to enter the pores without causing any size exclusion effects for either monomer or dimer forms of the drug.[9] Despite the slight difference in the SSA and total pore volume, the pore morphology can be considered similar between the two surface modifications, retaining its native fir-tree like structure, and allowing easy comparison of adsorption and confinement behavior of ibuprofen in THCPSi and TOPSi.

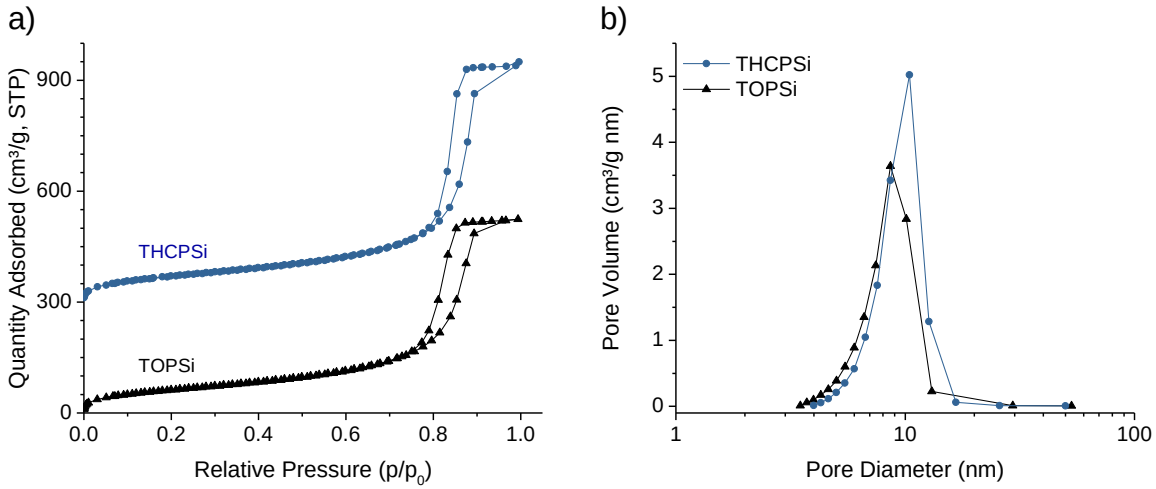

Figure 1. a) N_2 sorption isotherms and b) pore size distributions of THCPSi and TOPSi calculated from the isotherm adsorption branch using the BJH theory. The isotherms have been vertically shifted for clarity.

The chemical structure of the pore walls was studied with photoacoustic FTIR spectroscopy. Thermal oxidation at 300 °C replaces most of the native silicon hydrides with different Si−O structures. The TOPSi spectra shown in Figure 2 presents several features, such as broad bands centered around 1050 cm^{-1} and 1150 cm^{-1}, related to the surface Si−O−Si stretching modes, and another band at 2270 cm^{-1} related to the back-bond oxidized O_3−Si−H stretch.[38] A distinct feature also present in the spectra is a clear shoulder on the broad moisture related band at 3740 cm^{-1}, which can be assigned to O−H stretching vibrations of silanols (SiOH), providing possible groups for interaction with the adsorbate drug molecules.

The surface chemistry of THCPSi differs considerably from the more silica-like TOPSi. The hydrophobic nature of the initial PSi is retained, as the silicon hydrides are replaced with different hydrocarbon species using C_2H_2 as the hydrocarbon source. FTIR confirms the presence of different hydrocarbon structures through multiple absorbance peaks. In the high wavenumber region, the spectra are dominated by the strong symmetric and asymmetric stretching vibration bands related to C−H_x groups between 2850−2970 cm^{-1}, with an adjacent band at 3055 cm^{-1} that can be assigned to the =C−H stretching of vinyl groups. At lower wavenumbers, the different bending vibrations related to CH_2 and CH_3 can be

found between 1350−1470 cm^{-1}. Also present is a C=O stretching at 1715 cm^{-1}, which can be assigned to surface acyloxy groups. The lack of reactive or strongly polar surface groups makes THCPSi an ideal comparison partner to the partially silanol terminated TOPSi, as the possible interactions with the pore walls are very limited. The chemical stability of the THCPSi can also prevent possible unwanted reactions with the solvent molecules that could lead to surface oxidation.[39]

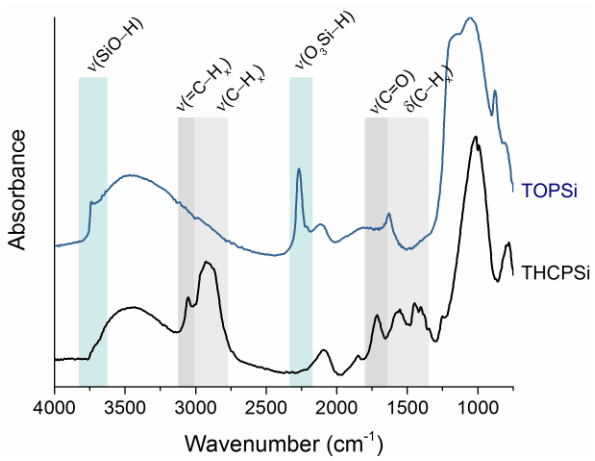

Figure 2. Photoacoustic FTIR spectra of TOPSi and THCPSi. The spectra have been vertically shifted for clarity.

3.2 Adsorption and Confinement of Ibuprofen

Particle immersion method was selected for the drug loading as it is easily controllable and allows facile sample preparation and handling. The main drawback of the method is the considerably larger consumption of the drug compared to**,** *e.g.***,** incipient wetness method, where the volume of the drug solution is comparable to the total pore volume of the adsorbent particles and to more advanced methods such as rotary evaporator or fluid bed -based loading.[40,41] Another low drug consumption approach is the melt method, where the drug is heated above its melting point allowing adsorption into the pores to take place. [42] For the loading tests, ibuprofen was dissolved into EtOH, THF or CHF, representing a polar protic, polar aprotic, and a nonpolar solvent, respectively. The properties of the solvents and the visually observed saturation solubilities of ibuprofen are listed in Table S1 (Supporting information). The selection of the solvents was made to allow evaluation of possible competitive adsorption between the

solvent and the solute with the pore surfaces**,** which could lead to differences in the drug payload. The immersion duration for the adsorption process was 2 h, as it was confirmed to be sufficient for obtaining a similar drug payload as longer immersions**,** by testing the three solvents and both particle types (Figure S2).

The microparticles of both surface chemistries were loaded using the same drug-particle ratios as permitted by the saturation solubilities across the three solvents, enabling the comparison in the efficiency of the loading and the effect of the selected surface chemistry. The total payload of adsorbed drug in the samples was determined with TG analysis. As this does not separate whether the drug has been confined into the mesopores or recrystallized onto the outer surfaces of the microparticles, DSC measurements were also carried out on each sample. Since crystalline ibuprofen melts at ca. 77 °C (Figure S3), its presence on the loaded samples can readily be observed from the respective thermograms of the loaded samples.[26,43] The amount of drug corresponding to the detected enthalpy of fusion was then subtracted from the total amount of ibuprofen, yielding the actual confined pore payload.

Figure 3 presents the obtained total drug amounts with the actual confined payloads normalized to the available pore volumes of the respective particle types. The results showed each solvent to be suitable for achieving high drug payloads, as the maximum ibuprofen amounts reached well over 1300 mg/cm^3 with THCPSi and ca. 1500 mg/cm^3 with TOPSi. When taking into account the external crystallization of ibuprofen, the amount of drug actually residing inside the mesopores was considerably lower, reaching a maximum of 800–850 mg/cm^3 with either surface chemistry as the loading solution concentration reached 400 mg/mL, corresponding to 8:1 (w/w) drug−PSi ratio. As the true density of ibuprofen is 1.11 g/cm^3,[44] the obtained confined payloads were ~75% from the theoretical maximum.

At higher concentrations, the amount of ibuprofen recrystallizing onto the particle external surfaces progressively increased. Surprisingly, the amount of confined ibuprofen appears to reduce at the highest concentrations of CHF and THF, indicating that some of the recrystallized drug may have originated due to the nucleation occurring during loading process on the particle external surfaces, hindering further ibuprofen diffusion into the mesopores. Despite the rapidly increasing recrystallized portion at higher

solution concentrations, high confined payload levels appeared to be reachable without causing excessive surface recrystallization of the drug. Optimally selecting the loading solution drug−PSi ratio also avoids the need for a rinsing step which can cause unwanted drug release.[40,45,46]

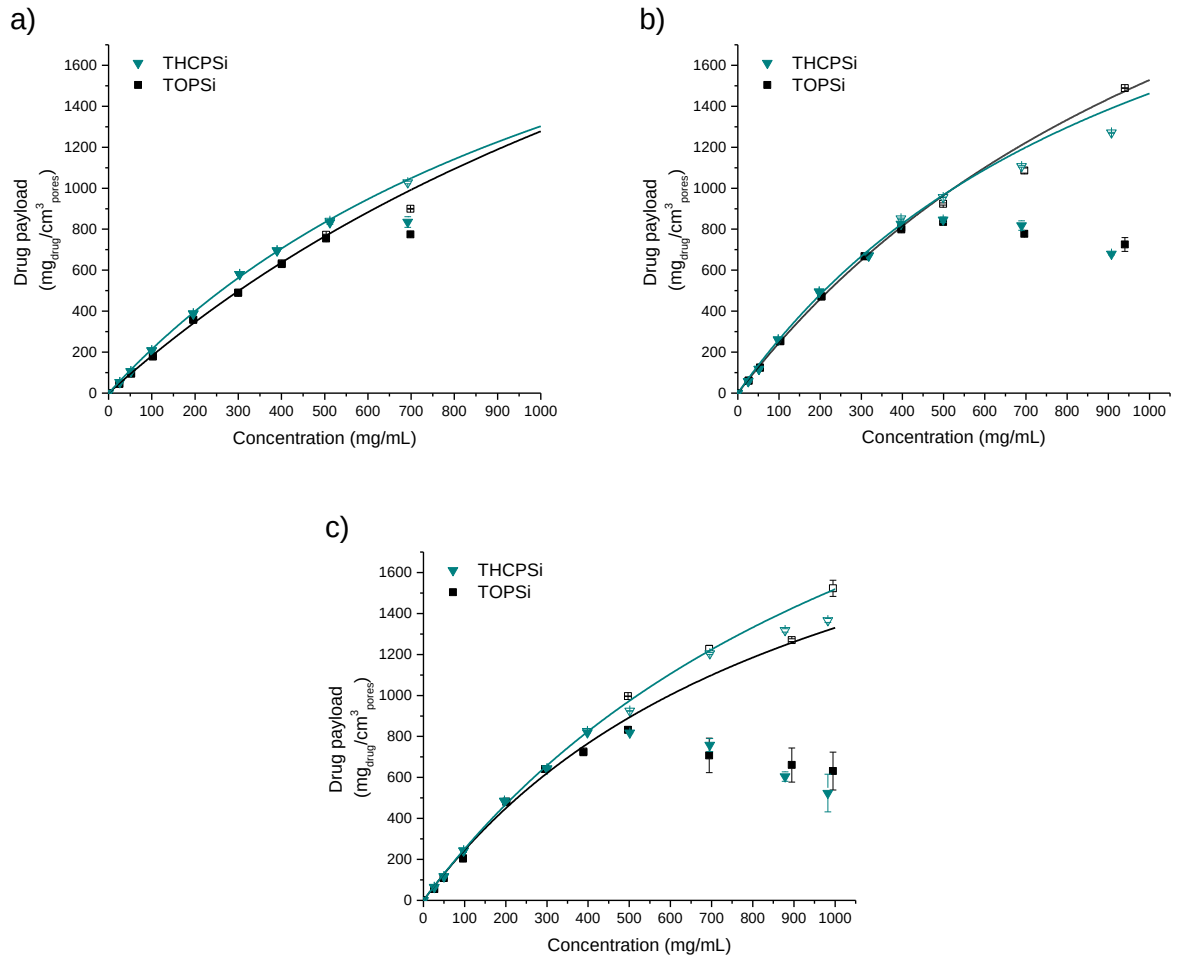

Figure 3. Adsorption of ibuprofen into TOPSi and THCPSi from a) EtOH, b) CHF, and c) THF. The open symbols show the total amount of ibuprofen adsorbed on the sample and the solid symbols the amount of drug confined into the pores. The solid lines were drawn to guide the eye.

Earlier studies have shown the selection of the loading solvent to have a considerable effect on the adsorption outcome.[40,47,48] With ibuprofen, solvents with lower dielectric constant appeared more preferable than solvents with a higher value providing higher drug payloads.[47] Comparing directly the

results, it could be seen that the intake of ibuprofen into the TOPSi or THCPSi particles was practically similar with all the solvents. The differences between solvents, however, were notable as would have been expected due to the differences in the solvent properties. Adsorption from the solvents with lower permittivity, CHF and THF, appeared to be more effective into TOPSi than from EtOH, as the difference between payloads, before the surface crystallization takes place, increased to ca. 130 mg/cm^3 with THF and 170 mg/cm^3 using CHF. With THCPSi, the differences between the solvents were smaller, as THF and CHF showed only ca. 110 mg/cm^3 higher drug payload, before the surface crystallization onset.

The slightly lower adsorption efficiency of ibuprofen into TOPSi using EtOH may be related to the possible intermolecular interactions between the drug and the solvent, and between the solvent and the partially silanol terminated TOPSi surface. The possible hydrogen bonding between EtOH and the pore surface may compete at lower ibuprofen concentrations with the drug adsorption. Hydrogen bonding of EtOH with drug monomers can also occur, and it has been shown to affect the recrystallization kinetics of ibuprofen.[49]

Interestingly, the DSC results from the EtOH based loadings presented in Figure 4 show broad endotherms well below the bulk melting temperature of ibuprofen beginning to appear at fairly low drug payloads of ca. 200 mg/cm^3, in both THCPSi and TOPSi. This may indicate that after the initial adsorption has taken place, the effect of the pore walls to the outcome is reduced, and solvent-drug interactions take precedence during the process. The formation of small crystallites with notable melting point depression according to the Gibbs-Thomson equation within the mesopores appeared very similar with all the solvents as these results were also seen with the loadings made from THF and CHF solutions, as shown in Figure S4.[43] The broad nature of the endotherms indicates the presence of various sizes of crystallites in mesoconfinement, with THCPSi showing a more distinct separation into two peaks at the higher drug payloads. Earlier studies conducted with ibuprofen confined into PSi of various pore sizes indicated that a pseudoliquid δ-layer is formed between the pore walls and the crystallites nucleated within the core region.[35] Also shown, was that the reduction of the crystal sizes did not appear to significantly reduce the enthalpy of fusion of the mesoconfined ibuprofen crystallites. The enthalpies of

the broad ibuprofen endotherms within the pores would then correspond 50–60 % of the actual pore payload, after the drug amount had reached over 300 mg/cm^3. This shows the high tendency of ibuprofen to crystallize even as the dimensions of the pores compared to the drug molecule itself are roughly only 10× its size. Similar size differences with PSi or silica pores using the drugs griseofulvin and indomethacin, however, did not cause any crystallization, indicating the sensitivity of the system to the used drug molecule.[50,51]

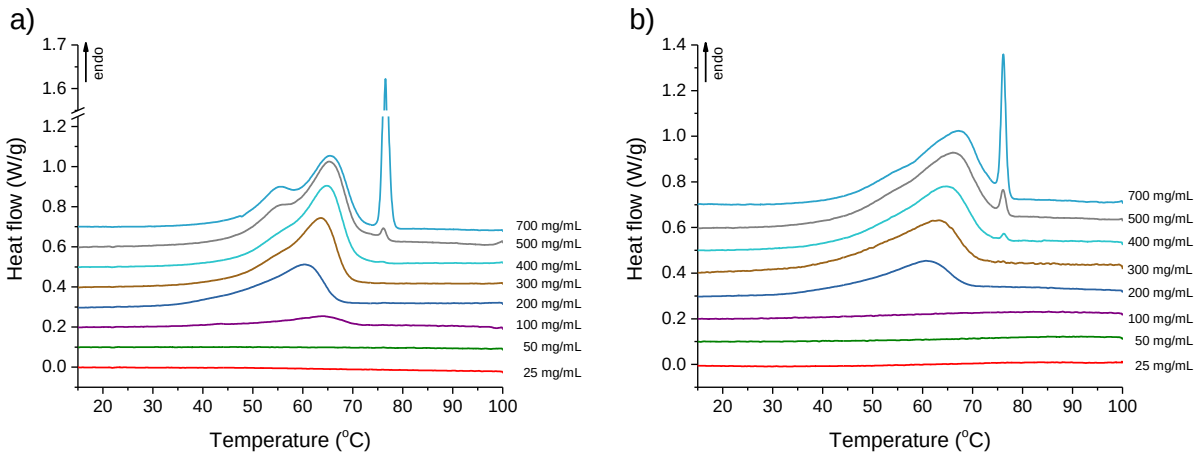

Figure 4. Heat flow curves of a) THCPSi and b) TOPSi samples loaded with ibuprofen from EtOH solutions.

3.3 Spectroscopic Analysis of Confined Ibuprofen

The slight differences in adsorption efficiency prompted further analysis on the ibuprofen loaded TOPSi and THCPSi samples. The presence of two phases of adsorbed ibuprofen, crystalline and non-crystalline, according to the DSC results, also warranted additional information on the molecular dynamics of the drug inside the confined matrix. FTIR and variable temperature NMR spectroscopy were employed to determine possible interactions between the adsorbed molecules and the pore walls.

A key difference between TOPSi and THCPSi is their surface chemistry. Oxidized PSi provides a hydrophilic and polar surface where silanol groups are present, whereas the hydrocarbonized PSi appears more nonpolar, providing few or no chemical groups capable of functioning as, *e.g.*, hydrogen bond

acceptors or donors. Ibuprofen, containing a carboxylic acid group, can function both as an acceptor or donor for multiple hydrogen bonds, tending also to be present in its dimeric form.[52]

The FTIR spectrum of crystalline ibuprofen is shown in Figure S5. It exhibits a fingerprint region comprising of multiple absorbance bands, along with a distinct band assigned to the C=O stretching of the carboxylic acid at 1705 cm^{-1}. After the adsorption of ibuprofen into PSi, despite the differences in the payloads between the solvents, the IR spectra appear quite similar. Figure 5 presents the carbonyl region FTIR spectra of samples loaded from several different concentrations of ibuprofen in EtOH (carbonyl region spectra of samples loaded from CHF and THF along with the full IR spectra, are shown in Figures S6 and S7). With both TOPSi and THCPSi, the spectra show the initial buildup of ibuprofen within the pores, when the immersion was done with 1:2 and 1:1 drug–PSi ratios and, as the pores were nearly filled with the drug, without excessive surface crystallization taking place (4:1 and 10:1 drug–PSi ratios). As the confined ibuprofen payload increases, the C=O stretch becomes more distinguishable. The main peak appears consistently at 1710 cm^{-1}, but seems to have a broadened toward higher wavenumbers at lower payloads. This slight shift indicates that hydrogen bonding between the ibuprofen dimers is weaker or broken up due to the presence of non-crystalline drug.[53] With THCPSi, the contribution from the acyloxy group emphasizes the main peak that can be assigned for the dimerized form of ibuprofen, hindering the interpretation of the stretching band. Partially, the presence of the non-crystalline ibuprofen in the pores leads to the widening of the band, but in the case of TOPSi, the effect of the silanol groups cannot be discounted.

With the samples containing only low amounts of ibuprofen, much of the features of the TOPSi spectra can still be easily resolved. Comparison of the silanol peak absorbance to the back-bond oxidized hydride stretching at 2260 cm^{-1} provided an effective point of reference, as the hydride group can be assumed not to take part in the possible hydrogen bonding between the pore walls and adsorbed ibuprofen molecules. The ratio of ν(SiO–H) and ν(O_3Si–H) decreased from 0.53 of pristine TOPSi to 0.37 and 0.25, corresponding to payloads of 45 mg/cm^3 and 95 mg/cm^3 of ibuprofen obtained with 1:2 and 1:1 drug–PSi ratios, respectively. This suggests that the reduction in the peak absorbance was not due to the increasing

amount of ibuprofen masking the spectral features, the ratio of ν(O_3Si–H) and ν(Si–O–Si) bands appeared to remain constant. This result indicates that the surface silanols actively take part in breaking up the ibuprofen dimers and can provide an attractive surface site for adsorption. Similar results have been confirmed computationally with ordered mesoporous silica,[54,55] showing the similarity of TOPSi and silica materials.

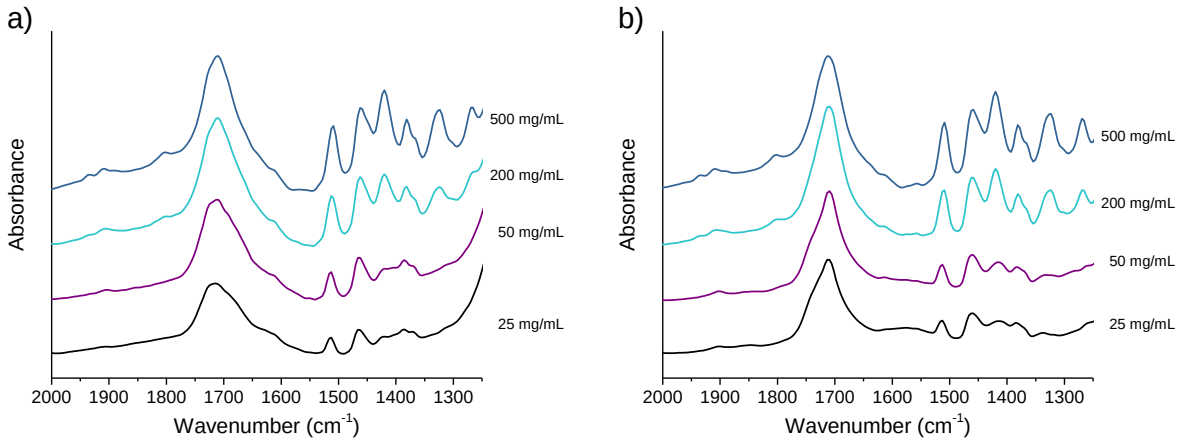

Figure 5. Photoacoustic FTIR spectra of the carbonyl stretching region of a) TOPSi and b) THCPSi microparticles loaded using ibuprofen-EtOH solutions.

Further confirmation of the ibuprofen-silanol interaction was sought with ^{1}H MAS NMR measurements at different sample temperatures. For the NMR measurements, we opted to use only the samples loaded with EtOH solution at 10:1 drug–PSi ratio (750 mg/cm^3 and 830 mg/cm^3 confined drug payloads for TOPSi and THCPSi, respectively), as the selected parameters provided a high payload of drug with only low ibuprofen surface recrystallization. At room temperature and at low MAS rates, the ^{1}H MAS spectra of samples with both the surface chemistries showed a broad baseline hump, typical for solid materials superimposed with several broad peaks due to the presence of a more mobile phase, causing averaging of the ^{1}H–^{1}H dipolar couplings, as shown in Figure S8. With a higher MAS rate, the actual temperature of the samples was increased to 55 °C, partially melting some of the confined drug. However, the peak separation was enhanced considerably due to the increased mobility of the molecules and the further suppression of the anisotropic broadening. The transverse relaxation time T_2 determined from the proton

resonance at ~1.3 ppm also showed a large difference in drug mobility, as the T_2 values ranged from 0.13 ms for crystalline ibuprofen to 6.3 and 7.4 ms for the non-crystalline drug within TOPSi and THCPSi pores, being comparable to values published earlier with similarly sized MCM-41.[22]

The differences between the TOPSi and THCPSi become evident in Figure 6. The contribution of the ibuprofen OH-group to the ^{1}H spectra can be seen in TOPSi as a very broad band around 9.4 ppm, while with THCPSi, the OH-related resonance peak is at considerably higher frequency at 12.3 ppm. These values show that when confined inside TOPSi, the more polar surface with silanol groups can disrupt some of the ibuprofen intermolecular hydrogen bonds in the liquid-like layer near the pore walls, through forming hydrogen bonds with free monomers. In addition, THCPSi does not provide similar sites for interaction as was evident from the FTIR spectra. The ibuprofen molecules in the liquid phase retain their strong hydrogen bonds typical for cyclic dimers. However, the pore wall based hydrogen bonding does not extend the disruption very far, thus being unable to affect markedly the ibuprofen recrystallization in the core region of the pores.

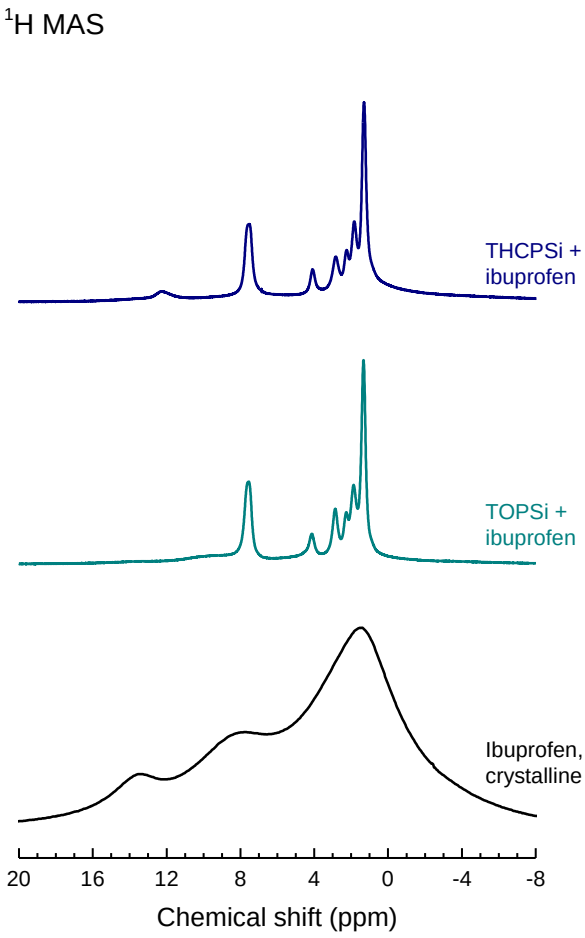

Figure 6. ^{1}H MAS NMR spectra of bulk crystalline ibuprofen with ibuprofen-loaded TOPSi and THCPSi obtained using a MAS rate ν_{MAS} = 14 kHz, with an effective sample temperature of 55 °C.

The samples were also studied using ^{13}C CP-MAS and direct MAS measurements. For solid materials, cross-polarization (CP), where the spin polarization of ^{1}H is transferred to ^{13}C through ^{1}H–^{13}C dipolar coupling, is used to enhance the spectra. Conversely, if the molecular motion is high enough, the fast tumbling of the molecules is enough to average out the dipolar coupling, making CP-MAS detection of such molecules ineffective. Direct ^{13}C MAS experiment using short recycle delay between scans with weak ^{1}H decoupling power, however, can detect the mobile phase while attenuating the crystalline phase contribution due to saturation and line-broadening effects. Thus, it is possible to almost selectively measure the ^{13}C spectra of the solid and the more mobile drug phase with CP-MAS and MAS

measurements, respectively. Similar progression as in the DSC endotherms was also observable in the two NMR spectra when increasing the sample temperature until the all the confined drug had been molten.

The CP-MAS and MAS spectra of ibuprofen loaded TOPSi and THCPSi are presented in Figure 7 and Figure 8, while Figure S9 shows the CP-MAS spectra of crystalline ibuprofen with the resonance peak assignments. According to the DSC results, the confined ibuprofen is ca. 50% nanocrystalline, with the remaining molecules either in the pseudoliquid δ-layer or in disordered state within the pores. The same presence of the two distinct populations of drug molecules was seen in the NMR spectra. At the initial measurement temperature, clear CP-MAS spectra were obtained with broadened features, resembling closely the bulk crystalline form of the drug. As with the ^{1}H MAS spectra, the carboxylic acid moieties could be observed to be participating in cyclic dimers, as the C1 carbon resonance peak is located at 183.0 ppm, similarly to the bulk crystalline ibuprofen. The corresponding MAS spectra taken consequently presented also multiple clear peaks, albeit weak, due to the lower mobility of the ibuprofen molecules. The ibuprofen C1 carbon resonance in TOPSi was shown to be more shielded as it resides at 180.1 ppm, indicating that some of the dimers are cleaved and the monomers could be hydrogen bonded to the surface silanols, while the corresponding resonance in THCPSi could be found at 180.7 ppm. The liquid-like behavior was also seen in the isobutyl chain resonance peak, as C13 carbon could now rotate freely becoming equivalent with the C12 carbon, causing the peak at 25.0 ppm in the CP-MAS spectra to weaken, with both the carbons contributing to the resonance peak at 21.8 ppm in the MAS spectra.

Increasing temperature showed the diminishing of the CP-MAS resonances with the reduction of the nanocrystalline phase, while in turn the MAS spectra becomes consistently stronger. As features in the CP-MAS spectra became practically indistinguishable after 63 °C, the corresponding liquid phase spectra showed little changes aside resonance intensity. The C1 carbon resonance appeared to be deshielded slightly as the resonance was shifted to 181.0 ppm with both surface chemistries.

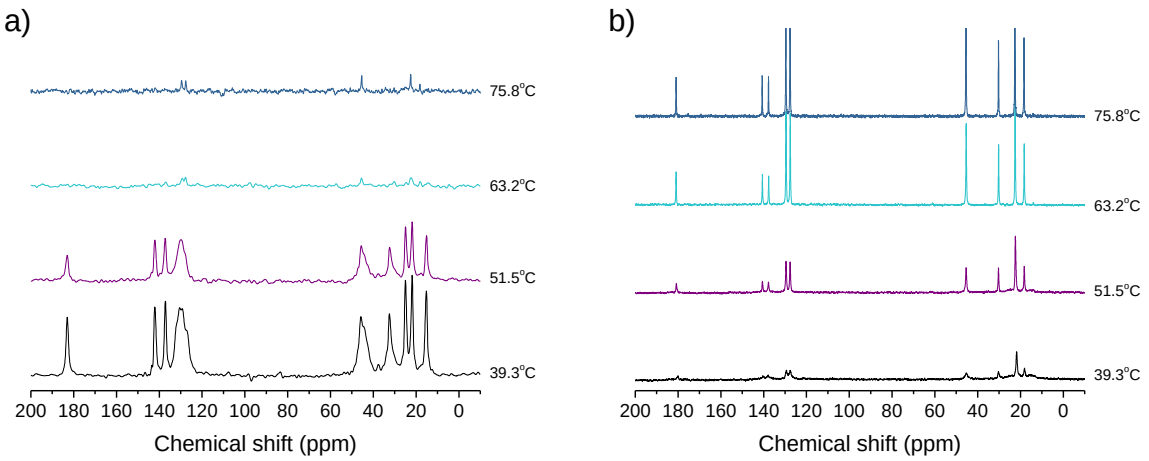

Figure 7. a) ^{13}C CP-MAS and b) ^{13}C MAS NMR spectra of ibuprofen confined in TOPSi. The variable temperature spectra were obtained using MAS rates of ν_{MAS} = 10 kHz, except for the highest temperature where ν_{MAS} = 12 kHz.

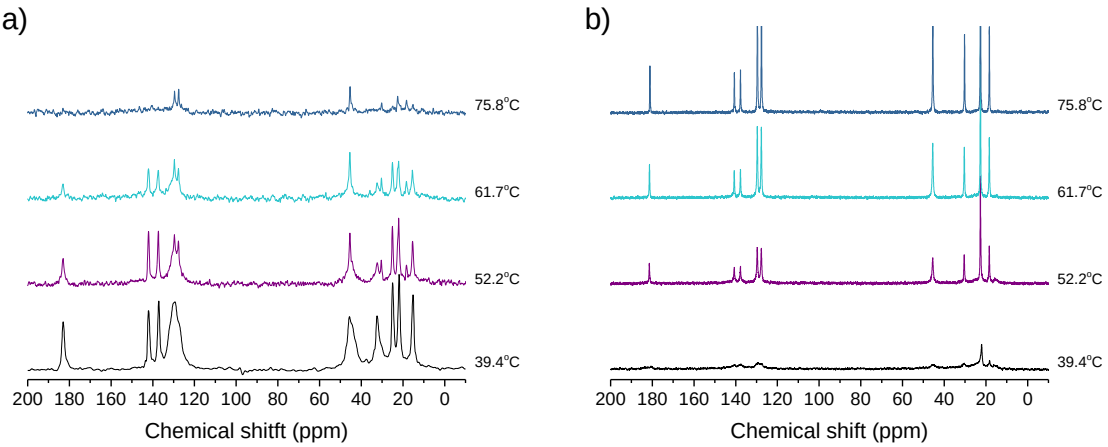

Figure 8. a) ^{13}C CP-MAS and b) ^{13}C MAS NMR spectra of ibuprofen confined in THCPSi. The variable temperature spectra were obtained using MAS rates of ν_{MAS} = 12 kHz, except for the lowest temperature where ν_{MAS} = 10 kHz.

3.4 Permeation Studies

The enhanced solubility of ibuprofen released from mesoporous materials has been well established using either porous silicon or silica.[10,56] While ibuprofen is classified having good permeability according to the Biopharmaceutical Classification System (BCS, Class II), possible effects caused by the hydrophobic THCPSi surface chemistry, with a WCA of 110° compared to 25° of TOPSi, and the presence of a nanocrystalline phase in the loaded particle types provided interest for permeation testing. The permeability tests were done using two model cell lines that simulate the conditions in the small intestine**,** where the systemic absorption of orally administered drug mainly takes place. Cell lines Caco-2 and co-culture of Caco-2/HT29 were selected to mimic intestinal conditions *in vitro*. The main difference in the two cell lines is the added mucus layer formed on the co-culture due to the addition of HT29 goblet cells to the model.[57]

The samples utilized in the permeation experiments were the same as used in the NMR measurements, exhibiting both high confined drug payload with a minimal amount of ibuprofen recrystallized on the particle external surfaces (10:1 drug−PSi ratio, EtOH solution). In order to contrast the ibuprofen permeation profiles with and without the presence of nanocrystalline drug within the pores, comparison samples were heated for 10 min at 75 °C prior to the permeability experiments. As ibuprofen recrystallization within the pores is slow, the immediate use of the microparticles provided a completely non-crystalline comparison. The permeation rates of the PSi microparticle samples and crystalline ibuprofen reference in Figure 9 showed only little difference between the samples when using the Caco-2/HT29 co-culture monolayers. As ibuprofen is a well permeable drug, its adsorption into microparticles was not expected to change its behavior drastically. The complete liquefaction of ibuprofen from the mesopores neither has a significant effect on the permeation outcome, even though both the liquefied samples showed slightly faster permeation. Similar results for the microparticles were obtained with plain Caco-2 line, as shown in Figure S10. With both the cell lines, the wetting of the particles also appeared very efficient, as the hydrophobic THCPSi behaved very comparably to its hydrophilic counterpart.

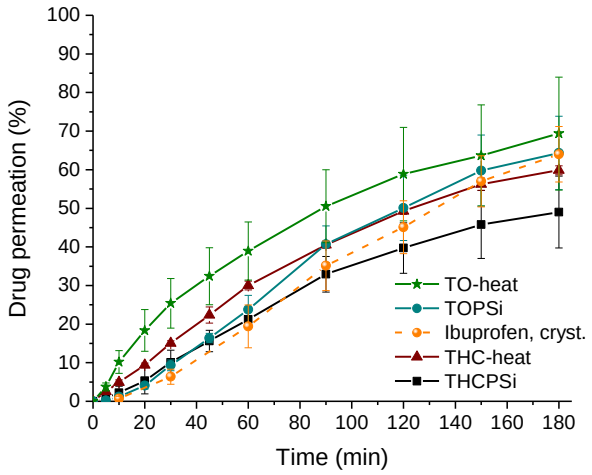

Figure 9. Permeation of TOPSi and THCPSi loaded and crystalline ibuprofen across Caco-2/HT29 monolayers at the apical and basolateral pH 7.4. The heated samples were placed in an oven at 75 °C for 10 min prior to the experiment in order to melt the nanocrystalline ibuprofen inside the mesopores.

4 Conclusions

The differences in molecular dynamics caused by the change of porous carrier or its properties emphasize the need for careful analysis in every individual case, as the drug behavior is not always fully predictable. Here, we have shown that immersion loading can easily be used to find suitable parameters to maximize the confined payload, while keeping the amount of external recrystallization very low, preventing the need for cumbersome rinsing steps after the loading. The overall influence of silanol groups and the polar nature of the TOPSi pore wall chemistry appeared to be quite limited on the ibuprofen adsorption and confinement. Even moderate drug payloads showed the tendency of the drug to form nanocrystalline structure within the pores. This confirms the fact that the extent of interactions does not affect beyond the initial layers adjacent to the pore walls, and at the core region the ibuprofen molecules are associated in dimer structures in both TOPSi and THCPSi. As PSi allows easy surface chemistry modification into either hydrophilic or hydrophobic directions, this prompts further investigations using drug molecules with tendency to form polymorphs to determine if the pore structure

and controlled interactions between the pore walls and the adsorbed molecules could further be exploited in crystal engineering for polymorph selection and stabilization.

ASSOCIATED CONTENT

Supporting Information. Experimental details; SEM images of particles and PSi layer cross-section; Solvent properties and ibuprofen apparent solubilities; immersion duration effects on payload; DSC heat flow curves of crystalline ibuprofen and loaded particles; FTIR spectra of crystalline ibuprofen; FTIR spectra of the carbonyl region of the loaded particles and the full spectra; ^{1}H MAS NMR spectra of crystalline and loaded ibuprofen; ^{13}C CP-MAS spectra of crystalline ibuprofen; permeation profiles of loaded ibuprofen across Caco-2 monolayers. This material is available free of charge via the Internet at http://pubs.acs.org.

AUTHOR INFORMATION

Corresponding Author

*E-mail: jarno.salonen@utu.fi

ACKNOWLEDGMENT

Dr. H. A. Santos acknowledges financial support from the Academy of Finland (decision nos. 252215 and 281300), the University of Helsinki Research Funds, the Biocentrum Helsinki, and the European Research Council under the European Union's Seventh Framework Programme (FP/2007–2013, Grant No. 310892). Mr. Arthur Bidois is acknowledged for the temperature calibrations of the solid-state NMR. This work made use of the Aalto University Nanomicroscopy Center (Aalto-NMC) premises.

REFERENCES

(1) Leuner, C.; Dressman, J. Improving Drug Solubility for Oral Delivery Using Solid Dispersions. *Eur. J. Pharm. Biopharm.* **2000**, *50*, 47–60.

(2) Vasconcelos, T.; Marques, S.; das Neves, J.; Sarmento, B. Amorphous Solid Dispersions: Rational Selection of a Manufacturing Process. *Adv. Drug Deliv. Rev.* **2016**, *100*, 85–101.

(3) Blagden, N.; de Matas, M.; Gavan, P. T.; York, P. Crystal Engineering of Active Pharmaceutical Ingredients to Improve Solubility and Dissolution Rates. *Adv. Drug Deliv. Rev.* **2007**, *59*, 617–630.

(4) Laitinen, R.; Löbmann, K.; Strachan, C. J.; Grohganz, H.; Rades, T. Emerging Trends in the Stabilization of Amorphous Drugs. *Int. J. Pharm.* **2013**, *453*, 65–79.

(5) Van Eerdenbrugh, B.; Van den Mooter, G.; Augustijns, P. Top-down Production of Drug Nanocrystals: Nanosuspension Stabilization, Miniaturization and Transformation into Solid Products. *Int. J. Pharm.* **2008**, *364*, 64–75.

(6) Corma, A. From Microporous to Mesoporous Molecular Sieve Materials and Their Use in Catalysis. *Chem. Rev.* **1997**, *97*, 2373–2420.

(7) Jane, A.; Dronov, R.; Hodges, A.; Voelcker, N. H. Porous Silicon Biosensors on the Advance. *Trends Biotechnol.* **2009**, *27*, 230–239.

(8) Gardner, D. S.; Holzwarth, C. W.; Liu, Y.; Clendenning, S. B.; Jin, W.; Moon, B.-K.; Pint, C.; Chen, Z.; Hannah, E. C.; Chen, C.; Wang, C; Mäkilä, E.; Chen, R.; Aldridge, T.; Gustafson, J. L. Integrated on-Chip Energy Storage Using Passivated Nanoporous-Silicon Electrochemical Capacitors. *Nano Energy* **2016**, *25*, 68–79.

(9) Vallet-Regi, M.; Rámila, A.; del Real, R. P.; Pérez-Pariente, J. A New Property of MCM-41: Drug Delivery System. *Chem. Mater.* **2001**, *13*, 308–311.

(10) Salonen, J.; Laitinen, L.; Kaukonen, A. M.; Tuura, J.; Björkqvist, M.; Heikkilä, T.; Vähä-Heikkilä, K.; Hirvonen, J.; Lehto, V.-P. Mesoporous Silicon Microparticles for Oral Drug Delivery: Loading and Release of Five Model Drugs. *J. Control. Release* **2005**, *108*, 362–374.

(11) Van Speybroeck, M.; Barillaro, V.; Thi, T. Do; Mellaerts, R.; Martens, J.; Van Humbeeck, J.; Vermant, J.; Annaert, P.; Van den Mooter, G.; Augustijns, P. Ordered Mesoporous Silica Material SBA-15: A Broad-Spectrum Formulation Platform for Poorly Soluble Drugs. *J. Pharm. Sci.* **2009**, *98*, 2648–2658.

(12) Kaukonen, A. M.; Laitinen, L.; Salonen, J.; Tuura, J.; Heikkilä, T.; Limnell, T.; Hirvonen, J.; Lehto, V.-P. Enhanced in Vitro Permeation of Furosemide Loaded into Thermally Carbonized Mesoporous Silicon (TCPSi) Microparticles. *Eur. J. Pharm. Biopharm.* **2007**, *66*, 348–356.

(13) Wang, F.; Hui, H.; Barnes, T. J.; Barnett, C.; Prestidge, C. A. Oxidized Mesoporous Silicon Microparticles for Improved Oral Delivery of Poorly Soluble Drugs. *Mol. Pharmaceutics* **2010**, *7*, 227–236.

(14) Bimbo, L. M.; Mäkilä, E.; Raula, J.; Laaksonen, T.; Laaksonen, P.; Strommer, K.; Kauppinen, E. I.; Salonen, J.; Linder, M. B.; Hirvonen, J.; Santos, H. A. Functional Hydrophobin-Coating of Thermally Hydrocarbonized Porous Silicon Microparticles. *Biomaterials* **2011**, *32*, 9089–9099.

(15) Kovalainen, M.; Mönkäre, J.; Mäkilä, E.; Salonen, J.; Lehto, V.-P.; Herzig, K.-H.; Järvinen, K. Mesoporous Silicon (PSi) for Sustained Peptide Delivery: Effect of PSi Microparticle Surface Chemistry on Peptide YY3-36 Release. *Pharm. Res.* **2012**, *29*, 837–846.

(16) Na, H.-K.; Kim, M.-H.; Park, K.; Ryoo, S.-R.; Lee, K. E.; Jeon, H.; Ryoo, R.; Hyeon, C.; Min, D.-H. Efficient Functional Delivery of siRNA Using Mesoporous Silica Nanoparticles with Ultralarge Pores. *Small* **2012**, *8*, 1752–1761.

(17) Schlipf, D. M.; Rankin, S. E.; Knutson, B. L. Pore-Size Dependent Protein Adsorption and Protection from Proteolytic Hydrolysis in Tailored Mesoporous Silica Particles. *ACS Appl. Mater. Interfaces* **2013**, *5*, 10111–10117.

(18) Tzur-Balter, A.; Shatsberg, Z.; Beckerman, M.; Segal, E.; Artzi, N. Mechanism of Erosion of Nanostructured Porous Silicon Drug Carriers in Neoplastic Tissues. *Nat. Commun.* **2015**, *6*, 6208.

(19) Wang, M.; Hartman, P. S.; Loni, A.; Canham, L. T.; Bodiford, N.; Coffer, J. L. Influence of Surface Chemistry on the Release of an Antibacterial Drug from Nanostructured Porous Silicon. *Langmuir* **2015**, *31*, 6179–6185.

(20) Kiwilsza, A.; Pajzderska, A.; Mielcarek, J.; Jenczyk, J.; Wąsicki, J. Dynamical Properties of Nimodipine Molecules Confined in SBA-15 Matrix. *Chem. Phys.* **2016**, *475*, 126–130.

(21) Mellaerts, R.; Roeffaers, M. B. J.; Houthoofd, K.; Van Speybroeck, M.; De Cremer, G.; Jammaer, J. A. G.; Van den Mooter, G.; Augustijns, P.; Hofkens, J.; Martens, J. A. Molecular Organization of Hydrophobic Molecules and Co-Adsorbed Water in SBA-15 Ordered Mesoporous Silica Material. *Phys. Chem. Chem. Phys.* **2011**, *13*, 2706–2713.

(22) Azaïs, T.; Tourné-Péteilh, C.; Aussenac, F.; Baccile, N.; Coelho, C.; Devoisselle, J.-M.; Babonneau, F. Solid-State NMR Study of Ibuprofen Confined in MCM-41 Material. *Chem. Mater.* **2006**, *18*, 6382–6390.

(23) Sciacca, B.; Secret, E.; Pace, S.; Gonzalez, P.; Geobaldo, F.; Quignard, F.; Cunin, F. Chitosan-Functionalized Porous Silicon Optical Transducer for the Detection Ofcarboxylic Acid-Containing Drugs in Water. *J. Mater. Chem.* **2011**, *21*, 2294–2302.

(24) Wu, E. C.; Andrew, J. S.; Cheng, L.; Freeman, W. R.; Pearson, L.; Sailor, M. J. Real-Time Monitoring of Sustained Drug Release Using the Optical Properties of Porous Silicon Photonic Crystal Particles. *Biomaterials* **2011**, *32*, 1957–1966.

(25) Alba-Simionesco, C.; Coasne, B.; Dosseh, G.; Dudziak, G.; Gubbins, K. E.; Radhakrishnan, R.; Sliwinska-Bartkowiak, M. Effects of Confinement on Freezing and Melting. *J. Phys. Condens. Matter* **2006**, *18*, R15–R68.

(26) Ha, J. M.; Wolf, J. H.; Hillmyer, M. A.; Ward, M. D. Polymorph Selectivity under Nanoscopic Confinement. *J. Am. Chem. Soc.* **2004**, *126*, 3382–3383.

(27) Ha, J. M.; Hamilton, B. D.; Hillmyer, M. A.; Ward, M. D. Alignment of Organic Crystals under Nanoscale Confinement. *Cryst. Growth Des.* **2012**, *12*, 4494–4504.

(28) Mellaerts, R.; Jammaer, J. A. G.; Van Speybroeck, M.; Chen, H.; Van Humbeeck, J.; Augustijns, P.; Van den Mooter, G.; Martens, J. A. Physical State of Poorly Water Soluble Therapeutic Molecules Loaded into SBA-15 Ordered Mesoporous Silica Carriers: A Case Study with Itraconazole and Ibuprofen. *Langmuir* **2008**, *24*, 8651–8659.

(29) Azaïs, T.; Hartmeyer, G.; Quignard, S.; Laurent, G.; Babonneau, F. Solution State NMR Techniques Applied to Solid State Samples: Characterization of Benzoic Acid Confined in MCM-41. *J. Phys. Chem. C* **2010**, *114*, 8884–8891.

(30) Aiello, D.; Folliet, N.; Laurent, G.; Testa, F.; Gervais, C.; Babonneau, F.; Azaïs, T. Solid State NMR Characterization of Phenylphosphonic Acid Encapsulated in SBA-15 and Aminopropyl-Modified SBA-15. *Microporous Mesoporous Mater.* **2013**, *166*, 109–116.

(31) Izquierdo-Barba, I.; Sousa, E.; Doadrio, J. C.; Doadrio, A. L.; Pariente, J. P.; Martínez, A.; Babonneau, F.; Vallet-Regí, M. Influence of Mesoporous Structure Type on the Controlled Delivery of Drugs: Release of Ibuprofen from MCM-48, SBA-15 and Functionalized SBA-15. *J. Sol-Gel Sci. Technol.* **2009**, *50*, 421–429.

(32) Brás, A. R.; Fonseca, I. M.; Dionísio, M.; Schönhals, A.; Affouard, F.; Correia, N. T. Influence of Nanoscale Confinement on the Molecular Mobility of Ibuprofen. *J. Phys. Chem. C* **2014**, *118*, 13857–13868.

(33) Jarvis, K. L.; Barnes, T. J.; Prestidge, C. A. Surface Chemistry of Porous Silicon and Implications for Drug Encapsulation and Delivery Applications. *Adv. Colloid Interface Sci.* **2012**, *175*, 25–38.

(34) Secret, E.; Wu, C.-C.; Chaix, A.; Galarneau, A.; Gonzalez, P.; Cot, D.; Sailor, M. J.; Jestin, J.; Zanotti, J.-M.; Cunin, F.; Coasne, B. Control of the Pore Texture in Nanoporous Silicon via Chemical Dissolution. *Langmuir* **2015**, *31*, 8121–8128.

(35) Riikonen, J.; Mäkilä, E.; Salonen, J.; Lehto, V.-P. Determination of the Physical State of Drug Molecules in Mesoporous Silicon with Different Surface Chemistries. *Langmuir* **2009**, *25*, 6137–6142.

(36) Neue, G.; Dybowski, C. Determining Temperature in a Magic-Angle Spinning Probe Using the Temperature Dependence of the Isotropic Chemical Shift of Lead Nitrate. *Solid State Nucl. Magn. Reson.* **1997**, *7*, 333–336.

(37) Tahvanainen, M.; Rotko, T.; Mäkilä, E.; Santos, H. A.; Neves, D.; Laaksonen, T.; Kallonen, A.; Hämäläinen, K.; Peura, M.; Serimaa, R.; Salonen, J.; Hirvonen, J.; Peltonen, L. Tablet Preformulations of Indomethacin-Loaded Mesoporous Silicon Microparticles. *Int. J. Pharm.* **2012**, *422*, 125–131.

(38) Mawhinney, D. B.; Glass, J. A.; Yates, J. T. FTIR Study of the Oxidation of Porous Silicon. *J. Phys. Chem. B* **1997**, *101*, 1202–1206.

(39) Salonen, J.; Björkqvist, M.; Laine, E.; Niinistö, L. Stabilization of Porous Silicon Surface by Thermal Decomposition of Acetylene. *Appl. Surf. Sci.* **2004**, *225*, 389–394.

(40) Charnay, C.; Bégu, S.; Tourné-Péteilh, C.; Nicole, L.; Lerner, D. A.; Devoisselle, J. M. Inclusion of Ibuprofen in Mesoporous Templated Silica: Drug Loading and Release Property. *Eur. J. Pharm. Biopharm.* **2004**, *57*, 533–540.

(41) Limnell, T.; Santos, H. A.; Mäkilä, E.; Heikkilä, T.; Salonen, J.; Murzin, D. Y.; Kumar, N.; Laaksonen, T.; Peltonen, L.; Hirvonen, J. Drug Delivery Formulations of Ordered and Nonordered Mesoporous Silica: Comparison of Three Drug Loading Methods. *J. Pharm. Sci.* **2011**, *100*, 3294–3306.

(42) Wang, M.; Coffer, J. L.; Dorraj, K.; Hartman, P. S.; Loni, A.; Canham, L. T. Sustained Antibacterial Activity from Triclosan-Loaded Nanostructured Mesoporous Silicon. *Mol. Pharmaceutics* **2010**, *7*, 2232–2239.

(43) Lehto, V.-P.; Vähä-Heikkilä, K.; Paski, J.; Salonen, J. Use of Thermoanalytical Methods in Quantification of Drug Load in Mesoporous Silicon Microparticles. *J. Therm. Anal. Calorim.* **2005**, *80*, 393–397.

(44) Rasenack, N.; Müller, B. W. Properties of Ibuprofen Crystallized under Various Conditions: A Comparative Study. *Drug Dev. Ind. Pharm.* **2002**, *28*, 1077–1089.

(45) O'Mahony, M.; Leung, A. K.; Ferguson, S.; Trout, B. L.; Myerson, A. S. A Process for the Formation of Nanocrystals of Active Pharmaceutical Ingredients with Poor Aqueous Solubility in a Nanoporous Substrate. *Org. Process Res. Dev.* **2015**, *19*, 1109–1118.

(46) Heikkilä, T.; Salonen, J.; Tuura, J.; Kumar, N.; Salmi, T.; Murzin, D. Y.; Hamdy, M. S.; Mul, G.; Laitinen, L.; Kaukonen, A. M.; Hirvonen, J.; Lehto, V.-P. Evaluation of Mesoporous TCPSi, MCM-41, SBA-15, and TUD-1 Materials as API Carriers for Oral Drug Delivery. *Drug Deliv.* **2007**, *14*, 337–347.

(47) Fernández-Núñez, M.; Zorrilla, D.; Montes, A.; Mosquera, M. J. Ibuprofen Loading in Surfactant-Templated Silica: Role of the Solvent according to the Polarizable Continuum Model. *J. Phys. Chem. A* **2009**, *113*, 11367–11375.

(48) Fisher, K. A.; Huddersman, K. D.; Taylor, M. J. Comparison of Micro- and Mesoporous Inorganic Materials in the Uptake and Release of the Drug Model Fluorescein and Its Analogues. *Chem. - A Eur. J.* **2003**, *9*, 5873–5878.

(49) Garekani, H. A.; Sadeghi, F.; Badiee, A.; Mostafa, S. A.; Rajabi-Siahboomi, A. R. Crystal Habit Modifications of Ibuprofen and Their Physicomechanical Characteristics. *Drug Dev. Ind. Pharm.* **2001**, *27*, 803–809.

(50) Mäkilä, E.; Ferreira, M. P. A.; Kivelä, H.; Niemi, S.; Correia, A.; Shahbazi, M.-A.; Kauppila, J.; Hirvonen, J.; Santos, H. A.; Salonen, J. Confinement Effects on Drugs in Thermally Hydrocarbonized Porous Silicon. *Langmuir* **2014**, *30*, 2196–2205.

(51) Ukmar, T.; Čendak, T.; Mazaj, M.; Kaučič, V.; Mali, G. Structural and Dynamical Properties of Indomethacin Molecules Embedded within the Mesopores of SBA-15: A Solid-State NMR View. *J. Phys. Chem. C* **2012**, *116*, 2662–2671.

(52) Carignani, E.; Borsacchi, S.; Geppi, M. Detailed Characterization of the Dynamics of Ibuprofen in the Solid State by a Multi-Technique NMR Approach. *ChemPhysChem* **2011**, *12*, 974–981.

(53) Kazarian, S. G.; Andrew Chan, K. L. "Chemical Photography" of Drug Release. *Macromolecules* **2003**, *36*, 9866–9872.

(54) Skorupska, E.; Jeziorna, A.; Paluch, P.; Potrzebowski, M. J. Ibuprofen in Mesopores of Mobil Crystalline Material 41 (MCM-41): A Deeper Understanding. *Mol. Pharmaceutics* **2014**, *11*, 1512–1519.

(55) Delle Piane, M.; Corno, M.; Pedone, A.; Dovesi, R.; Ugliengo, P. Large-Scale B3LYP Simulations of Ibuprofen Adsorbed in MCM-41 Mesoporous Silica as Drug Delivery System. *J. Phys. Chem. C* **2014**, *118*, 26737–26749.

(56) Andersson, J.; Rosenholm, J.; Areva, S.; Lindén, M. Influences of Material Characteristics on Ibuprofen Drug Loading and Release Profiles from Ordered Micro- and Mesoporous Silica Matrices. *Chem. Mater.* **2004**, *16*, 4160–4167.

(57) Liu, D.; Bimbo, L. M.; Mäkilä, E.; Villanova, F.; Kaasalainen, M.; Herranz-Blanco, B.; Caramella, C. M.; Lehto, V.-P.; Salonen, J.; Herzig, K.-H.; Hirvonen, J.; Santos, H. A. Co-Delivery of a Hydrophobic Small Molecule and a Hydrophilic Peptide by Porous Silicon Nanoparticles. *J. Control. Release* **2013**, *170*, 268–278.

For Table of Contents Only